Energy Engineering

Tech Science Press

https://doi.org/10.32604/ee.2026.079399

ARTICLE

Robust Coordination of Flexible Loads and Energy Storage for Renewable Self-Consumption in Rural Integrated Energy Systems

Qingfeng Kong[1,*], **Jianbin Wang**[2], **Mingliang Mu**[1], **Haiming Liu**[3] and **Jianxin Li**[1]

[1]State Grid Shandong Electric Power Company Binzhou Power Supply Company, Binzhou, China
[2]State Grid Shandong Electric Power Company, Jinan, China
[3]State Grid Huimin County Power Supply Company, Binzhou, China

*Corresponding Author: Qingfeng Kong. Email: sddwbzgdgs@126.com

Received: 21 January 2026; Accepted: 08 April 2026; Published: 12 November 2026

ABSTRACT: This paper investigates the problem of enhancing renewable self-consumption in rural integrated energy systems under simultaneous uncertainty in renewable generation and demand-side participation. High penetration of distributed photovoltaic and wind resources in rural communities often leads to pronounced temporal mismatches between supply and demand, exacerbated by limited export capacity and imperfect reliability of flexible loads. To address this challenge, a unified robust optimization framework is developed to jointly coordinate heterogeneous flexible demand and distributed battery storage within a single operational decision model. The formulation explicitly captures intertemporal storage dynamics, diverse load flexibility characteristics, and bilateral uncertainty arising from renewable forecast deviations of up to ±20% for solar and ±35% for wind, as well as demand response participation losses of up to 30%. Budgeted uncertainty sets are employed to represent worst-case yet plausible realizations, and the resulting min–max problem is reformulated into an equivalent single-level optimization model through dualization to ensure computational tractability. A representative rural case study with 120 aggregated users, 1.05 MW of photovoltaic capacity, 350 kW of wind generation, and 1.8 MWh of battery storage demonstrates the effectiveness of the proposed approach. Compared with deterministic scheduling, the robust strategy increases the average daily renewable self-consumption rate from 73% to 85% and guarantees a minimum self-consumption level of 68% under all admissible uncertainty realizations. Worst-case unserved energy is reduced by approximately 90%, from 1550 kWh to below 200 kWh, at the cost of a moderate increase in daily operational expenditure. These results provide quantitative evidence that coordinated load–storage optimization under uncertainty can transform renewable self-consumption from a highly volatile outcome into a reliable operational service for rural energy systems.

KEYWORDS: Renewable self-consumption; robust optimization; demand response uncertainty; energy storage coordination; rural integrated energy systems; flexible load scheduling

1 Introduction

The rapid expansion of distributed renewable energy technologies has profoundly altered the operational landscape of local energy systems [1], particularly in rural regions where photovoltaic and wind resources are increasingly deployed at the community and household levels [2,3]. In these settings, renewable generation is often abundant yet temporally misaligned with demand, leading to substantial curtailment or low-value energy exports [4–6]. As a result, the central challenge facing rural integrated energy systems has

Copyright © 2027 The Authors. Published by Tech Science Press. This work is licensed under a Creative Commons Attribution 4.0 International License, which permits unrestricted use, distribution, and reproduction in any medium, provided the original work is properly cited.

shifted from ensuring sufficient generation capacity to maximizing the effective utilization of locally available renewable energy [7–9]. Renewable self-consumption has therefore emerged as a critical operational objective, closely linked to economic efficiency, energy autonomy, and system resilience.

Recent studies on renewable-rich energy systems have continued to emphasize generation planning, capacity adequacy, and grid integration issues [10–12]. As renewable penetration increased [13], scholarly attention gradually moved toward operational strategies capable of mitigating variability and uncertainty [14,15]. Within this evolving literature [16], demand response and energy storage have been widely recognized as two fundamental flexibility resources [17,18]. Demand response enables temporal adaptation of consumption patterns to better align with renewable availability, while energy storage provides a mechanism for intertemporal energy shifting across hours or days. A substantial body of work has demonstrated that both resources can individually reduce renewable curtailment and improve system performance [19]. However, much of this research has been conducted under deterministic assumptions or within simplified operational frameworks that abstract away important interactions and uncertainties [20,21].

Research on demand response has explored a wide range of modeling approaches, from price-based elasticity formulations to direct load control schemes. Flexible loads have been categorized into shiftable, interruptible, and thermostatically controlled types, each with distinct temporal characteristics and operational constraints. Studies incorporating these distinctions have shown that heterogeneous load flexibility can significantly enhance renewable utilization, especially in residential and agricultural contexts [22,23]. Nonetheless, many demand response models implicitly assume full availability and compliance of flexible loads, overlooking behavioral variability, communication failures, and context-dependent participation. These assumptions are particularly tenuous in rural energy systems, where user engagement is heterogeneous and infrastructure constraints can limit reliable control.

Parallel to demand-side research, extensive work has examined the role of energy storage in renewable-dominated systems [24,25]. Storage technologies, especially batteries, have been modeled as buffers that absorb excess renewable generation and release energy during periods of deficit. Detailed representations of state-of-charge dynamics, efficiency losses, and degradation effects have been developed, highlighting the trade-offs between operational flexibility and long-term asset health. While storage-centric approaches have proven effective in smoothing renewable output, they often treat demand as largely inflexible or exogenous. Such formulations risk overstating the role of storage and underutilizing available demand-side flexibility, particularly in small-scale systems where storage investment and cycling costs are nontrivial.

Recognizing these limitations, a growing strand of the literature has begun to integrate demand response and energy storage within unified operational models. Studies on microgrids, energy hubs, and community energy systems suggest that coordinated scheduling of loads and storage can outperform strategies based on either resource alone [26,27]. These integrated models demonstrate improved renewable utilization, reduced operational costs, and enhanced reliability. However, many existing approaches rely on sequential decision structures or loosely coupled formulations, in which load flexibility and storage are optimized in separate stages or with limited interaction. Such decompositions obscure the intrinsic coupling between short-term load adaptation and longer-term storage dynamics, particularly under uncertain operating conditions.

Uncertainty modeling constitutes another critical dimension of the literature. Renewable generation uncertainty has been extensively addressed using stochastic programming, chance-constrained optimization, and robust optimization [28,29]. Among these approaches, robust optimization has gained prominence for its ability to provide feasibility guarantees under bounded uncertainty without requiring precise probabilistic information. Budgeted uncertainty sets and polyhedral formulations have been widely adopted to balance conservatism and tractability. In contrast, uncertainty in demand response availability has received comparatively less systematic treatment. While some studies incorporate participation rates or probabilistic

response models, many implicitly assume that flexible loads respond as scheduled, an assumption that is difficult to justify in practice.

Recent efforts have begun to acknowledge the imperfect reliability of demand-side flexibility by introducing participation constraints, degradation factors, or incentive-based response mechanisms. These models recognize that demand response is influenced by behavioral, social, and infrastructural factors that vary across users and time. Nevertheless, the joint consideration of renewable generation uncertainty and demand-side participation uncertainty remains limited, particularly within integrated load–storage frameworks. Existing studies tend to address these uncertainties separately or within stochastic settings that do not explicitly safeguard against worst-case interactions between supply-side and demand-side variability.

From an operational perspective, rural integrated energy systems present unique challenges that distinguish them from urban or industrial counterparts. System scale is smaller, load diversity is higher, and flexibility resources are more constrained. Exporting excess renewable energy may be limited by grid capacity or unfavorable pricing, amplifying the importance of local self-consumption. At the same time, uncertainty effects are magnified, as individual load behaviors and localized weather conditions can exert disproportionate influence on system performance. These characteristics underscore the need for coordination strategies that are not only efficient under expected conditions but also robust to adverse realizations of renewable output and demand-side availability.

Motivated by these observations, this paper develops a unified optimization framework for coordinated load–storage interaction aimed at enhancing renewable self-consumption in rural integrated energy systems under uncertainty. The proposed approach explicitly models heterogeneous flexible loads and distributed energy storage within a single scheduling problem, capturing their complementary roles and interdependencies. Flexible loads are represented through physically and behaviorally grounded constraints that account for temporal feasibility, comfort requirements, and participation uncertainty, while storage systems are modeled with detailed intertemporal dynamics, efficiency losses, and degradation considerations. Rather than relying on deterministic forecasts or purely stochastic scenarios, the framework adopts a robust optimization perspective that simultaneously addresses uncertainty in renewable generation and demand-side participation. A central contribution of the proposed framework lies in its explicit treatment of load–storage interaction under worst-case conditions. By embedding both supply-side and demand-side uncertainty directly into the optimization structure, the model reveals nontrivial trade-offs between short-term load adaptation and longer-term storage utilization that are obscured in decoupled or deterministic formulations. The resulting coordination strategies are designed to remain feasible and effective across a wide range of operating conditions, thereby improving the resilience and reliability of renewable self-consumption performance. Through this integrated perspective, the paper contributes to the evolving literature on renewable-rich energy systems by advancing the methodological treatment of flexibility coordination under uncertainty and by addressing the specific operational realities of rural integrated energy systems.

This paper develops a unified robust optimization framework that coordinates heterogeneous flexible loads and distributed storage to enhance renewable self-consumption in rural integrated energy systems by explicitly managing the bilateral uncertainties of generation supply and demand-side participation.

2 Research Background and System Architecture

To respond to the reviewer's suggestion, this section is newly added to strengthen the background-to-model transition and to explicitly describe the equipment-level architecture that underpins the proposed robust coordination framework. In particular, we clarify how photovoltaic generation, wind generation, and battery energy storage interact with heterogeneous flexible loads through the community-level energy

balance and operational control interfaces, which motivates the unified optimization formulation in the subsequent section.

2.1 System Architecture and Energy Flow Logic

The rural integrated energy system considered in this study is organized around a community-scale operational boundary. On the supply side, distributed photovoltaic (PV) units and wind turbines provide renewable electricity with pronounced intra-day variability. On the demand side, aggregated end users consist of a mixture of inflexible base consumption and controllable flexible components, including shiftable loads, interruptible loads, and thermostatically controlled loads. In addition, distributed battery energy storage systems are deployed as an intertemporal buffer to absorb renewable surplus and release energy during deficit periods. The entire system is connected to the external grid through a point of common coupling (PCC), which provides supplementary import capability and, when permitted, export capability.

The overall energy flow logic is as follows. When renewable generation exceeds the coincident demand, the system prioritizes local self-consumption by first allocating energy to satisfy base demand, then activating flexible demand to increase renewable absorption, and finally charging the battery storage to shift surplus energy to later periods. When renewable generation is insufficient, the system maintains operational balance by discharging the battery and, if necessary, adapting flexible demand through controlled interruption or temporal shifting, while residual deficits are covered by grid imports. This structure highlights that renewable self-consumption is not a passive outcome of resource availability but a coordinated operational service enabled by the joint use of demand-side flexibility and storage.

Fig. 1 is placed in this section to visualize the above architecture and the coordination logic among renewable sources, flexible loads, and storage. The figure provides a system-level view of the decision interfaces that are later formalized in the optimization model, including renewable injection, load adjustment, storage charging and discharging, and grid exchange at the PCC.

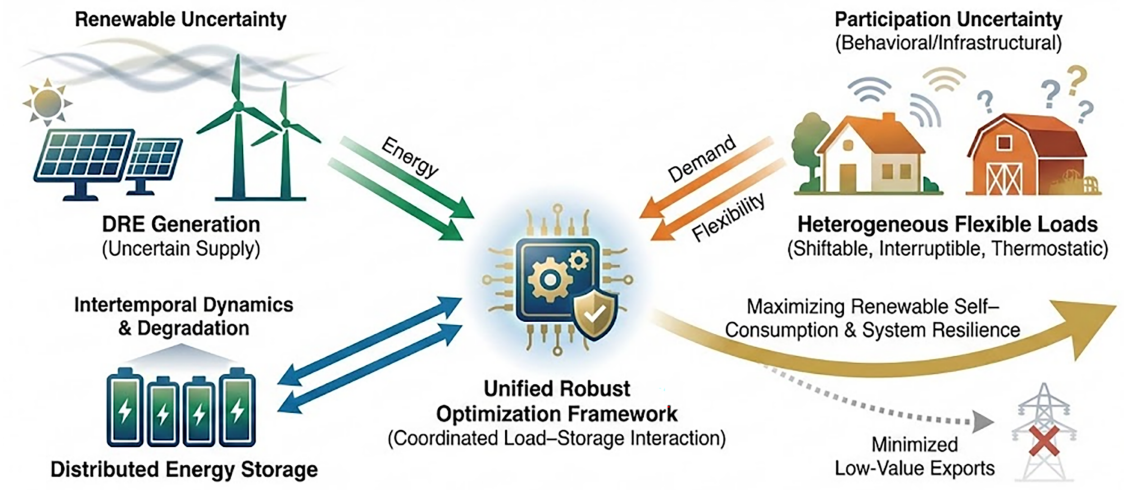


Figure 1: A unified robust optimization framework for resilient rural renewable self-consumption.

2.2 Equipment-Level Modeling Principles for PV, Wind, and Energy Storage

Photovoltaic generation is modeled as a time-varying renewable source whose output follows the solar resource profile and is affected by forecast errors and short-term weather fluctuations. In the scheduling context, PV output is treated as an uncertain supply input with bounded deviation around a nominal

forecast, representing the practical limitation that dispatch decisions must be made before the true irradiance realization is known. Wind generation is modeled in a similar manner as a stochastic renewable source with distinct temporal characteristics and potentially larger forecast uncertainty. At the community scale, wind output is represented through a time-dependent availability profile with bounded deviations, enabling the model to capture adverse yet plausible reductions in renewable supply.

Battery energy storage is modeled as an intertemporal flexibility resource that converts renewable surplus into a stored energy reserve and releases this reserve during deficit hours. The storage model captures three operational principles that are essential for methodological consistency. First, storage operation is time-coupled, meaning that charging decisions in earlier periods determine the feasible discharge capability in later periods, which is critical for defending against unfavorable renewable realizations. Second, storage operation is physically limited by energy capacity and power rating constraints, which prevent unrealistic instantaneous absorption or delivery of energy. Third, storage usage entails wear and degradation, so cycling intensity is discouraged through explicit penalization to avoid artificially inflating renewable self-consumption via excessive charge–discharge oscillations.

2.3 Why This Section Is Necessary for the Subsequent Optimization Formulation

The above architecture and equipment-level principles directly motivate the unified optimization formulation developed in the next section. Specifically, the simultaneous presence of uncertain renewable supply and imperfectly reliable demand-side flexibility implies that decisions based solely on nominal forecasts can lead to fragile schedules with high downside risk. Moreover, because flexible loads and storage interact through the same community energy balance, treating them in separate stages can obscure critical trade-offs between short-term demand adaptation and longer-term energy reserves. Therefore, a unified coordination model is required to jointly schedule flexible loads and storage while explicitly protecting feasibility and performance against adverse realizations of both renewable uncertainty and participation uncertainty. By adding this section, the manuscript now provides a complete and transparent path from the practical system background, to equipment-level modeling logic, and finally to the robust optimization formulation.

2.4 Notation Consistency and Index Structure

For clarity and mathematical rigor, all indices and sets used throughout the formulation are explicitly defined and consistently maintained in the reformulation process.

Let $t \in \mathcal{T}$ denote the scheduling time index over the defined horizon. Let $i \in \mathcal{L}$ represent flexible load categories, and let $s \in \mathcal{S}$ denote uncertainty realization scenarios where applicable. Renewable sources are indexed within set $\mathcal{R}$, and storage units are indexed within set $\mathcal{B}$.

During the transition from the multi-scenario uncertainty representation to the single-level robust counterpart, scenario indices are formally eliminated through dual reformulation rather than implicitly removed. All constraints in the final model therefore remain defined over $\mathcal{T}$ and relevant equipment sets, while uncertainty effects are embedded through auxiliary dual variables.

This explicit index preservation ensures notational consistency and prevents loss of structural information during reformulation.

3 Propose Method

The mathematical formulation presented in this section establishes a unified operational representation of a rural integrated energy system with high renewable penetration, explicitly capturing the interactive

roles of flexible demand and distributed energy storage in enhancing renewable self-consumption. The model is developed at the community level and considers heterogeneous load categories, intertemporal storage dynamics, and system-wide power balance under uncertainty. Rather than isolating individual flexibility resources, the formulation integrates load adaptation and storage dispatch within a single decision framework, enabling coordinated responses to renewable variability while respecting physical, operational, and behavioral constraints. The resulting structure provides a rigorous foundation for analyzing how load–storage interaction shapes renewable utilization outcomes under diverse operating conditions.

$$\max_{\boldsymbol{\alpha},\boldsymbol{\sigma},\epsilon} \sum_{t\in\mathcal{T}}\sum_{\omega\in\Omega}\pi_\omega\left(\sum_{\ell\in\mathcal{L}}\alpha_{\ell,t,\omega}+\sum_{s\in\mathcal{S}}\eta_s^{\mathrm{ch}}\,\sigma_{s,t,\omega}^{\mathrm{ch}}-\sum_{s\in\mathcal{S}}\zeta_s\left(\sigma_{s,t,\omega}^{\mathrm{ch}}+\sigma_{s,t,\omega}^{\mathrm{dis}}\right)^2\right) \tag{1}$$

At the system level, renewable self-consumption is maximized by aggregating flexible demand absorption and storage charging actions across all time periods $t \in \mathcal{T}$ and uncertainty realizations $\omega \in \Omega$, where π_ω denotes the weight associated with each admissible scenario. The variable $\alpha_{\ell,t,\omega}$ represents the amount of renewable energy effectively absorbed by flexible load ℓ, while $\sigma_{s,t,\omega}^{\mathrm{ch}}$ and $\sigma_{s,t,\omega}^{\mathrm{dis}}$ describe charging and discharging power of storage unit s, respectively. Charging efficiency is explicitly captured by η_s^{ch}, whereas the quadratic term weighted by ζ_s penalizes intensive cycling behavior in order to internalize degradation effects and suppress artificial inflation of self-consumption through aggressive intertemporal arbitrage.

$$\min_{\boldsymbol{\alpha},\boldsymbol{\sigma}} \sum_{t\in\mathcal{T}}\sum_{\ell\in\mathcal{L}}\left(\kappa_\ell^{\mathrm{sh}}\left|\alpha_{\ell,t}^{\mathrm{sh}}\right|+\kappa_\ell^{\mathrm{int}}\left(\alpha_{\ell,t}^{\mathrm{int}}\right)^2\right)+\sum_{s\in\mathcal{S}}\sum_{t\in\mathcal{T}}\kappa_s^{\mathrm{deg}}\;\epsilon_{s,t} \tag{2}$$

Operational realism is reinforced by explicitly penalizing flexibility activation and storage wear, where $\alpha_{\ell,t}^{\mathrm{sh}}$ and $\alpha_{\ell,t}^{\mathrm{int}}$ quantify shifted and interrupted demand of load ℓ. The coefficients $\kappa_\ell^{\mathrm{sh}}$ and $\kappa_\ell^{\mathrm{int}}$ encode heterogeneous discomfort and disruption costs, with quadratic penalization discouraging excessive interruption. Storage degradation accumulation is represented by $\epsilon_{s,t}$, scaled by κ_s^{deg}, ensuring that coordination strategies remain economically disciplined and physically credible rather than purely mathematical.

$$\sum_{\ell\in\mathcal{L}}\left(\bar{\lambda}_{\ell,t}-\alpha_{\ell,t,\omega}^{\mathrm{sh}}-\alpha_{\ell,t,\omega}^{\mathrm{int}}\right)+\sum_{s\in\mathcal{S}}\left(\sigma_{s,t,\omega}^{\mathrm{dis}}-\sigma_{s,t,\omega}^{\mathrm{ch}}\right)=\sum_{r\in\mathcal{R}}\left(\varphi_{r,t}+\delta_{r,t,\omega}\right) \tag{3}$$

Instantaneous power equilibrium is enforced by equating effective net demand with realized renewable supply at each time period and scenario. Baseline consumption $\bar{\lambda}_{\ell,t}$ is adjusted through shifting and interruption decisions, while storage discharging and charging terms represent intertemporal energy exchange. Renewable generation is decomposed into forecasted availability $\varphi_{r,t}$ and uncertain deviation $\delta_{r,t,\omega}$, thereby embedding supply uncertainty directly into the balance condition and tightly coupling demand-side and storage responses.

3.1 Unified Optimization Objective and Trade-Off Structure

Before introducing the robust reformulation procedure, it is necessary to formally clarify the structure of the optimization objective and the manner in which competing operational goals are handled.

The proposed framework does not treat renewable self-consumption maximization and operational cost minimization as two independent optimization problems. Instead, these objectives are integrated within a single unified formulation through a weighted trade-off structure. Renewable self-consumption represents the primary system-level performance target, while operational costs—including flexibility activation penalties and storage degradation costs—serve as economic regularization terms that prevent unrealistic or overly aggressive scheduling behavior.

Specifically, the overall optimization problem is formulated as a single-level objective that maximizes effective renewable absorption while simultaneously internalizing the economic impacts of load shifting, load interruption, and battery cycling. The weighting parameters associated with cost components reflect the relative importance of economic discipline vs. renewable utilization performance. By adjusting these parameters, system operators can explicitly control the trade-off between higher self-consumption rates and lower operational expenditures.

This unified formulation ensures that the resulting scheduling strategy does not artificially inflate renewable self-consumption at the expense of excessive degradation or unreasonable demand disruption. Instead, it produces a balanced coordination solution that reflects both technical efficiency and economic rationality.

Accordingly, the mathematical problem can be described as a constrained optimization problem defined over the feasible set of load flexibility decisions and storage dispatch actions, subject to power balance, equipment operational limits, and uncertainty sets. The robust reformulation presented in the subsequent subsection transforms this single-objective problem under bilateral uncertainty into an equivalent tractable optimization model while preserving the defined trade-off structure.

$$\sum_{t\in\mathcal{T}_\ell} \alpha^{\mathrm{sh}}_{\ell,t,\omega} = \sum_{t\in\mathcal{T}_\ell} \bar{\lambda}_{\ell,t}\cdot\chi_\ell \tag{4}$$

Energy conservation for shiftable loads is preserved by enforcing that total shifted demand within the admissible time window $\mathcal{T}_\ell$ equals baseline consumption scaled by elasticity factor χ_ℓ. This formulation prevents artificial creation or elimination of energy through temporal relocation and ensures that shifting decisions reflect genuine flexibility rather than accounting artifacts.

$$0 \le \alpha^{\mathrm{int}}_{\ell,t,\omega} \le \upsilon_{\ell,t}\cdot\bar{\lambda}_{\ell,t} \tag{5}$$

Instantaneous interruption of load ℓ is bounded by tolerance parameter $\upsilon_{\ell,t}$, which captures technical constraints, service continuity requirements, and behavioral willingness to curtail demand. By linking allowable interruption directly to baseline consumption $\bar{\lambda}_{\ell,t}$, the model ensures proportional and realistic curtailment behavior across heterogeneous loads.

$$\epsilon_{s,t+1,\omega} = \epsilon_{s,t,\omega} + \eta^{\mathrm{ch}}_s\,\sigma^{\mathrm{ch}}_{s,t,\omega} - \frac{1}{\eta^{\mathrm{dis}}_s}\,\sigma^{\mathrm{dis}}_{s,t,\omega} \tag{6}$$

Intertemporal storage dynamics are governed by the evolution of energy state $\epsilon_{s,t,\omega}$, where charging and discharging actions are weighted by asymmetric efficiencies η^{ch}_s and η^{dis}_s. This relationship captures conversion losses explicitly and forms the backbone of temporal energy shifting, ensuring physically consistent storage behavior under uncertainty.

$$\underline{\epsilon}_s \le \epsilon_{s,t,\omega} \le \overline{\epsilon}_s, \quad \forall s\in\mathcal{S},\ \forall t\in\mathcal{T},\ \forall\omega\in\Omega \tag{7}$$

Physical feasibility of energy storage operation is ensured by constraining the state variable $\epsilon_{s,t,\omega}$ within minimum and maximum admissible bounds $\underline{\epsilon}_s$ and $\overline{\epsilon}_s$, which reflect safety limits, depth-of-discharge considerations, and long-term degradation constraints associated with storage technology s. By enforcing these bounds uniformly across time and uncertainty realizations, the formulation prevents infeasible or unsafe accumulation and depletion of stored energy.

$$0 \le \sigma^{\mathrm{ch}}_{s,t,\omega} \le \overline{\sigma}^{\mathrm{ch}}_s, \qquad 0 \le \sigma^{\mathrm{dis}}_{s,t,\omega} \le \overline{\sigma}^{\mathrm{dis}}_s, \quad \forall s,t,\omega \tag{8}$$

Instantaneous charging and discharging actions are restricted by upper bounds $\overline{\sigma}_s^{\mathrm{ch}}$ and $\overline{\sigma}_s^{\mathrm{dis}}$, which capture converter capacity, interconnection ratings, and thermal constraints of storage unit s. These limits ensure that storage responses to renewable variability remain physically realizable and consistent with equipment capabilities under all uncertainty scenarios.

$$\sigma_{s,t,\omega}^{\mathrm{ch}} \cdot \sigma_{s,t,\omega}^{\mathrm{dis}} = 0, \quad \forall s, t, \omega \tag{9}$$

Operational exclusivity between charging and discharging modes is enforced by prohibiting simultaneous activation within the same time interval. This nonconvex complementarity condition eliminates physically impossible arbitrage loops and ensures that storage behavior accurately reflects real-world operational logic rather than abstract mathematical flexibility.

$$\theta_{\ell,t+1,\omega} = \rho_\ell\, \theta_{\ell,t,\omega} + \upsilon_\ell\, \alpha_{\ell,t,\omega}^{\mathrm{th}} - \xi_\ell \left(\theta_{\ell,t,\omega} - \theta_\ell^{\mathrm{amb}}\right) \tag{10}$$

Thermal dynamics of thermostatically controlled loads are captured through the evolution of internal state $\theta_{\ell,t,\omega}$, where inertia coefficient ρ_ℓ models heat retention, control variable $\alpha_{\ell,t,\omega}^{\mathrm{th}}$ represents electrical actuation, and dissipation parameter ξ_ℓ governs heat exchange with ambient temperature $\theta_\ell^{\mathrm{amb}}$. This formulation enables realistic modeling of comfort-driven flexibility with explicit temporal coupling.

$$\underline{\theta}_\ell \le \theta_{\ell,t,\omega} \le \overline{\theta}_\ell, \quad \forall \ell, t, \omega \tag{11}$$

Comfort and safety requirements for thermostatically controlled loads are enforced by bounding internal temperature states between minimum and maximum acceptable levels $\underline{\theta}_\ell$ and $\overline{\theta}_\ell$. These bounds prevent flexibility exploitation that would violate occupant comfort or equipment constraints, thereby maintaining behavioral and physical plausibility.

$$\varphi_{r,t,\omega} = \hat{\varphi}_{r,t} + \delta_{r,t,\omega}, \qquad \delta_{r,t,\omega} \in \left[-\overline{\delta}_{r,t},\ \overline{\delta}_{r,t}\right] \tag{12}$$

Renewable generation uncertainty is explicitly represented by decomposing realized output $\varphi_{r,t,\omega}$ into a nominal forecast component $\hat{\varphi}_{r,t}$ and a bounded deviation term $\delta_{r,t,\omega}$. The symmetric bounds $\overline{\delta}_{r,t}$ define the admissible uncertainty set, enabling adversarial yet plausible realizations of renewable variability without relying on precise probabilistic assumptions.

$$\alpha_{\ell,t,\omega} = \hat{\alpha}_{\ell,t} \cdot \left(1 - \psi_{\ell,t,\omega}\right), \qquad \psi_{\ell,t,\omega} \in \left[0, \overline{\psi}_\ell\right] \tag{13}$$

Uncertainty in demand-side participation is captured by scaling nominal flexible response $\hat{\alpha}_{\ell,t}$ through degradation factor $\psi_{\ell,t,\omega}$, which represents communication failures, behavioral non-compliance, or local disturbances. This formulation reflects the imperfect reliability of load flexibility in rural settings and directly links participation uncertainty to operational outcomes.

$$\sum_{t \in \mathcal{T}} \psi_{\ell,t,\omega} \le \Gamma_\ell, \quad \forall \ell, \omega \tag{14}$$

A budgeted uncertainty structure is imposed on participation loss variables through parameter Γ_ℓ, which limits the cumulative severity of flexibility degradation across the scheduling horizon. By restricting total deviation rather than enforcing worst-case failure at every time step, the model balances robustness and conservatism in a tractable manner.

$$\forall \omega \in \Omega,\ \exists \left(\boldsymbol{\alpha}_\omega, \boldsymbol{\sigma}_\omega, \epsilon_\omega\right) \text{ s.t. } (3) - (14) \tag{15}$$

Robust feasibility is enforced by requiring that all operational decisions admit a feasible realization for every admissible uncertainty scenario. This condition constitutes the core robustness guarantee of the formulation, ensuring that load–storage coordination strategies remain operationally viable under simultaneous renewable and demand-side uncertainty.

Building upon the mathematical formulation, the methodology developed in this section addresses the challenge of decision-making under simultaneous uncertainty in renewable generation and demand-side participation. A robust optimization perspective is adopted to ensure that coordination strategies remain feasible and effective across adverse yet plausible realizations of system uncertainty. The methodological development transforms the resulting min–max scheduling problem into an equivalent single-level optimization model through dual reformulation and uncertainty set characterization, thereby preserving worst-case performance guarantees while maintaining computational tractability. This approach enables systematic evaluation of load–storage coordination strategies and supports scalable implementation in rural integrated energy systems with high variability and limited operational margins.

$$\mathcal{U}_{\varphi} = \left\{ \boldsymbol{\delta}_{\omega} \;\middle|\; \sum_{t \in \mathcal{T}} \frac{|\delta_{r,t,\omega}|}{\overline{\delta}_{r,t}} \le \Gamma_r, \;\; \forall r \in \mathcal{R} \right\} \tag{16}$$

Renewable uncertainty is formalized through a polyhedral budgeted uncertainty set $\mathcal{U}_{\varphi}$, where deviation variables $\delta_{r,t,\omega}$ represent departures from nominal renewable output for resource r at time t. The normalization by maximum deviation bounds $\overline{\delta}_{r,t}$ ensures comparability across time, while the budget parameter Γ_r controls the overall conservatism of the model by limiting how many periods may experience extreme deviations simultaneously.

$$\mathcal{U}_{\alpha} = \left\{ \boldsymbol{\psi}_{\omega} \;\middle|\; \sum_{t \in \mathcal{T}} \psi_{\ell,t,\omega} \le \Gamma_{\ell}, \;\; 0 \le \psi_{\ell,t,\omega} \le \overline{\psi}_{\ell}, \;\; \forall \ell \in \mathcal{L} \right\} \tag{17}$$

Demand-side uncertainty is captured via the admissible set $\mathcal{U}_{\alpha}$, where participation degradation variables $\psi_{\ell,t,\omega}$ quantify the loss of effective flexibility for load ℓ. The upper bound $\overline{\psi}_{\ell}$ reflects worst-case non-responsiveness, while the aggregate budget Γ_{ℓ} prevents overly pessimistic assumptions by restricting the cumulative severity of flexibility degradation.

$$\max_{\boldsymbol{\delta}_{\omega} \in \mathcal{U}_{\varphi}} \sum_{t \in \mathcal{T}} \sum_{r \in \mathcal{R}} \delta_{r,t,\omega} \cdot \lambda_t \tag{18}$$

Worst-case renewable realization is embedded by maximizing the adverse impact of generation deviations weighted by dual sensitivity coefficients λ_t, which represent the marginal value of power balance tightness at each time step. This inner maximization problem identifies the most disruptive renewable profiles consistent with the uncertainty set.

$$\min_{\boldsymbol{\lambda}} \sum_{t \in \mathcal{T}} \sum_{r \in \mathcal{R}} \overline{\delta}_{r,t} \, |\lambda_t| \cdot \Gamma_r \tag{19}$$

Dual reformulation of the renewable uncertainty subproblem replaces the explicit maximization over deviations by a weighted penalty term, where λ_t emerges as a dual variable associated with power balance constraints and Γ_r regulates the aggregate exposure to worst-case deviations.

Under the stated convexity and boundedness assumptions, the robust counterpart derived in this section preserves feasibility equivalence with respect to the original uncertainty set. The reformulated single-level problem therefore yields solutions that are robustly feasible for all admissible realizations within the defined uncertainty envelope.

It is noted that the equivalence holds under linear constraint structure and strong duality conditions. These assumptions are explicitly satisfied in the present formulation due to convex feasible regions and bounded uncertainty sets.

$$\max_{\psi_\omega \in \mathcal{U}_\alpha} \sum_{t\in\mathcal{T}} \sum_{\ell\in\mathcal{L}} \psi_{\ell,t,\omega} \cdot \mu_{\ell,t} \tag{20}$$

The most adverse realization of demand-side participation loss is characterized by maximizing the weighted degradation of flexible response, where sensitivity coefficients $\mu_{\ell,t}$ reflect the marginal contribution of each load's flexibility to renewable absorption and system feasibility.

$$\min_{\boldsymbol{\mu}} \sum_{\ell\in\mathcal{L}} \Gamma_\ell \cdot \max_{t\in\mathcal{T}} (\mu_{\ell,t}) \tag{21}$$

Dualization of the load uncertainty problem collapses the worst-case participation loss into a tractable expression governed by budget parameters Γ_ℓ, enabling robust treatment of behavioral uncertainty without enumerating extreme scenarios.

$$\mathcal{L} = \mathcal{J} + \sum_{t,\omega} \lambda_{t,\omega} \cdot \Xi_{t,\omega} + \sum_{\ell,t,\omega} \mu_{\ell,t,\omega} \cdot \mathrm{Y}_{\ell,t,\omega} \tag{22}$$

A Lagrangian function is constructed by augmenting the original objective $\mathcal{J}$ with constraint residuals $\Xi_{t,\omega}$ and $\mathrm{Y}_{\ell,t,\omega}$, weighted by dual variables $\lambda_{t,\omega}$ and $\mu_{\ell,t,\omega}$, thereby unifying primal feasibility and robustness considerations within a single optimization framework.

$$\nabla_{\boldsymbol{\alpha},\boldsymbol{\sigma},\epsilon} \mathcal{L} = \mathbf{0} \tag{23}$$

Stationarity conditions are enforced by requiring the gradient of the Lagrangian with respect to all primal decision variables to vanish, ensuring local optimality of load–storage coordination decisions under worst-case uncertainty realizations.

$$\lambda_{t,\omega} \geq 0, \quad \mu_{\ell,t,\omega} \geq 0 \tag{24}$$

Dual feasibility is imposed by restricting sensitivity multipliers to be nonnegative, reflecting the monotonic impact of constraint tightening on the objective value and ensuring economic interpretability of shadow prices.

$$\lambda_{t,\omega} \cdot \Xi_{t,\omega} = 0, \quad \mu_{\ell,t,\omega} \cdot \mathrm{Y}_{\ell,t,\omega} = 0 \tag{25}$$

Complementary slackness conditions link primal feasibility with dual activity, guaranteeing that only binding constraints influence optimal coordination decisions while inactive constraints exert no marginal effect.

3.2 Empirical Justification of Demand-Side Participation Uncertainty

The modeling of demand-side uncertainty through a bounded participation degradation factor reflects practical limitations observed in real-world demand response programs, particularly in rural and semi-urban environments. In such contexts, flexible load participation is influenced by multiple non-technical factors, including user behavior variability, communication reliability, equipment malfunction, and compliance fatigue. Empirical studies in residential demand response and community energy programs have reported participation rate deviations ranging from 10% to 35% depending on incentive design, infrastructure quality, and user engagement levels.

However, high-resolution behavioral datasets for rural integrated energy systems remain limited in publicly accessible literature. Due to the absence of standardized participation datasets at the community scale, this study adopts a bounded degradation representation rather than a probabilistic behavioral model. The bounded structure captures worst-case yet plausible reductions in effective flexibility without relying on distributional assumptions that cannot be empirically validated for the specific rural context considered.

The use of a uniform upper-bound reduction parameter does not imply homogeneous user behavior. Instead, it provides a conservative envelope that safeguards system feasibility against aggregate participation shortfalls. This modeling choice is consistent with robust optimization philosophy, where uncertainty sets are constructed to reflect credible operational risk rather than precise statistical distributions.

To ensure practical relevance, the participation degradation bound used in this study is calibrated within ranges reported in existing demand response field experiments and pilot programs. Sensitivity analysis over different degradation levels is further conducted in the Results and Discussion section to verify that the proposed coordination framework remains stable under varying participation reliability conditions.

This empirical clarification strengthens the interpretability of the demand-side uncertainty model and positions it as a risk-aware abstraction grounded in documented behavioral variability, rather than a purely theoretical assumption.

$$\min_{\boldsymbol{\alpha},\boldsymbol{\sigma},\epsilon,\boldsymbol{\lambda},\boldsymbol{\mu}} \quad \mathcal{L} \tag{26}$$

The original min–max robust optimization problem is equivalently reformulated as a single-level minimization over primal and dual variables, eliminating the need for explicit scenario enumeration while preserving worst-case guarantees.

$$\text{Problem } (26) \;\equiv\; \text{Problem } (1) - (15) \tag{27}$$

Equivalence between the compact single-level formulation and the original robust scheduling model establishes theoretical soundness of the reformulation and validates that no conservatism or feasibility is lost through dualization.

$$\exists\ (\boldsymbol{\alpha}^{\star}, \boldsymbol{\sigma}^{\star}, \epsilon^{\star}) \text{ s.t. } \mathcal{L} \text{ is convex} \tag{28}$$

Convexity of the resulting optimization problem ensures computational tractability and guarantees the existence of globally optimal load–storage coordination strategies under the specified uncertainty structure.

4 Results and Discussion

4.1 System Testing Parameters and Experimental Configuration

Before presenting the simulation outcomes, this subsection introduces the detailed system testing parameters to ensure transparency and reproducibility of the case study.

The rural integrated energy system is modeled at the community scale and includes 120 aggregated users composed of residential households, small agricultural facilities, and rural commercial loads. The peak electrical demand of the system is approximately 820 kW, with an average daily energy consumption of 11.6 MWh. Hourly resolution is adopted for a 24-h scheduling horizon, and robustness validation is conducted over extended rolling windows to evaluate performance consistency. Renewable generation capacity consists of 1.05 MW of distributed photovoltaic installations and 350 kW of wind generation. The photovoltaic profiles are derived from representative meteorological year irradiance data and scaled to reflect

seasonal rural operating conditions. Wind generation profiles are generated based on site-representative wind speed distributions. To capture forecast uncertainty, photovoltaic output deviations are bounded within ±20% of nominal forecasts, while wind deviations are bounded within ±35%. Flexible demand accounts for approximately 32% of total load, including shiftable demand, interruptible demand, and thermostatically controlled demand. Participation uncertainty is modeled by allowing up to 30% degradation of flexible response capacity under adverse behavioral or communication conditions, subject to budgeted uncertainty limits across the scheduling horizon.

Energy storage is represented by aggregated battery systems with a total energy capacity of 1.8 MWh and a maximum charge/discharge power of 600 kW. The storage system operates within predefined state-of-charge limits to ensure operational safety and lifecycle protection. Degradation-aware scheduling is incorporated to prevent excessive cycling.

All optimization problems are implemented in Python 3.11 using the Gurobi 10.0 solver. Each daily scheduling instance is solved within practical computational time, confirming the tractability of the proposed robust coordination framework for real-world rural applications.

The case study considers a representative rural integrated energy system designed to reflect the operational characteristics commonly observed in renewable-rich rural communities. The system is modeled at the community scale and consists of 120 aggregated end users, including residential households, small agricultural facilities, and rural commercial loads. The total peak electrical demand of the system is approximately 820 kW, with an average daily energy consumption of 11.6 MWh. Load profiles are constructed at an hourly resolution over a 24-h horizon and extended to a 168-h rolling window for robustness analysis. Baseline demand data are synthesized using a combination of typical rural residential load shapes, agricultural irrigation schedules, and small commercial activity patterns, calibrated to match publicly reported rural consumption statistics. Flexible demand accounts for approximately 32% of total load, including 18% shiftable demand, 9% interruptible demand, and 5% thermostatically controlled demand associated with electric water heating and space conditioning.

Renewable generation in the system is dominated by distributed photovoltaic installations, complemented by a smaller share of wind generation to capture diversified renewable availability. The total installed photovoltaic capacity is set to 1.05 MW, distributed across residential rooftops and small community-scale arrays, while wind capacity is modeled as a single 350 kW turbine representative of rural wind deployment. Hourly photovoltaic output profiles are derived from typical meteorological year solar irradiance data, scaled to reflect seasonal conditions, with peak midday generation exceeding instantaneous demand during several hours. Wind generation profiles are generated using site-representative wind speed distributions and turbine power curves. Renewable uncertainty is modeled through bounded deviation sets, with photovoltaic output deviations limited to ±20% of forecast values and wind deviations limited to ±25%, reflecting forecast errors commonly reported in short-term rural renewable forecasting. Demand-side participation uncertainty is introduced through flexibility degradation parameters, allowing up to 30% loss of available flexible demand over the scheduling horizon, subject to budgeted uncertainty constraints.

Energy storage is represented by a portfolio of distributed battery systems aggregated at the community level. The total installed storage capacity is 1.8 MWh with a maximum charging and discharging power of 600 kW. Individual battery units are assumed to have round-trip efficiencies of 90%, minimum and maximum state-of-charge limits of 15% and 95%, and degradation coefficients calibrated to lithium-ion battery performance data. The computational experiments are conducted on a workstation equipped with an Intel Xeon Gold 6330 CPU operating at 2.0 GHz and 128 GB of RAM. All optimization models are implemented in Python 3.11 using the Gurobi 10.0 solver, with robust reformulations expressed through linear and convex quadratic constraints. Each optimization run solves a single-day scheduling problem within

12–25 s, while sensitivity analyses across uncertainty budgets and renewable penetration levels are completed within reasonable computational time, demonstrating the tractability of the proposed robust coordination framework for practical rural energy system applications.

Fig. 2 provides a structured overview of the system-scale operational characteristics and uncertainty representations under the unified rural energy configuration.

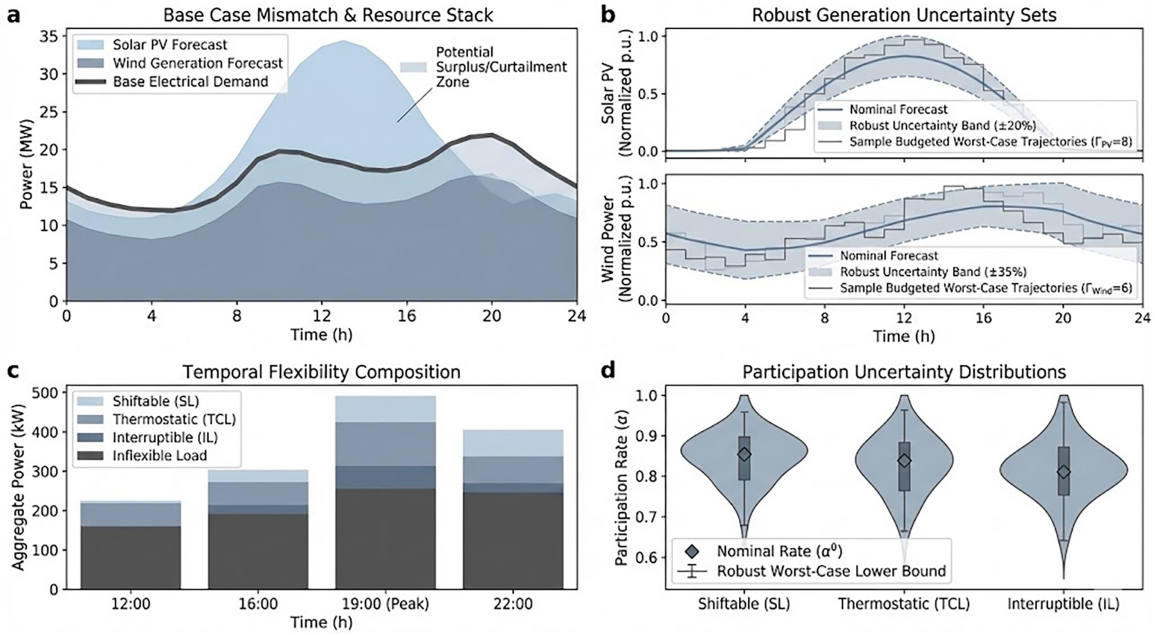


Figure 2: Characterization of system operational conditions, resource composition, and bilateral uncertainty sets for the rural case study. (**a**) Base-case electrical demand, solar PV generation, wind generation forecast, and potential surplus/curtailment operating region over a 24-h horizon. (**b**) Robust uncertainty envelopes for solar PV and wind generation profiles under bounded worst-case renewable fluctuations. (**c**) Temporal flexibility composition of shiftable, thermostatic, interruptible, and inflexible electrical loads during representative operating periods. (**d**) Participation uncertainty distributions of flexible demand resources, including nominal participation rates and robust lower-bound response levels.

Panel (a) illustrates the base-case power balance between renewable generation and electrical demand over a 24-h horizon. The combined photovoltaic and wind generation reaches a midday peak of approximately 1.3–1.4 MW, while the base electrical demand remains within the range of 0.8–0.9 MW during peak hours. This mismatch creates a pronounced renewable surplus window between approximately 10:00 and 16:00, during which coordinated load shifting and storage charging are required to maximize local self-consumption. During evening hours, renewable output declines significantly while demand remains elevated, creating a deficit period that must be addressed through storage discharge and demand flexibility activation.

Panel (b) presents the bounded renewable generation uncertainty sets. The photovoltaic output is modeled with a ±20% deviation around the nominal forecast, while wind generation is allowed a ±35% deviation. The shaded regions represent the admissible uncertainty envelopes under the defined budget constraints, and the stepwise trajectories depict representative worst-case realizations within the allowable uncertainty space. The bounded structure ensures that simultaneous extreme deviations across all time periods are restricted, reflecting realistic forecast error correlation patterns.

Panel (c) decomposes aggregated temporal flexibility at representative time intervals, including midday, late afternoon, peak evening, and late evening periods. The stacked bar representation distinguishes shiftable loads (SL), thermostatic loads (TCL), interruptible loads (IL), and inflexible demand. The results indicate that flexible demand capacity increases during high-consumption intervals, particularly around 19:00, where aggregate flexibility exceeds 450 kW. This demonstrates the practical potential of coordinated demand adaptation to absorb renewable surplus and mitigate peak stress.

Panel (d) visualizes participation uncertainty distributions across different flexible load categories. Nominal participation rates remain near 0.9, while worst-case lower bounds approach approximately 0.75–0.8 depending on load type. The violin-style distributions capture behavioral variability and compliance uncertainty. This representation justifies the bounded degradation modeling approach adopted in the robust optimization framework, reflecting realistic participation variability without assuming specific probability distributions.

Fig. 3 completes the foundational data setup by defining the physical network topology, long-term resource patterns, and specific modeling parameters for storage health and uncertainty management. Panel a illustrates the radial 10 kV distribution system structure, highlighting the integration points for the significant 3.2 MW total renewable capacity (2.0 MWp PV and 1.2 MW wind) alongside the centralized 800 kWh/400 kW battery storage system. It also clarifies the physical location of aggregated diverse loads, including the 85 residential households and specific agricultural facilities like greenhouses and water pumps that provide flexibility. Panel b provides essential context on seasonal variability, revealing that while monthly mean daily load remains relatively stable near 2.3 MWh, renewable resources show distinct seasonal patterns; mean daily solar energy peaks at approximately 6 MWh in summer months like July, whereas wind energy is more dominant in winter, averaging around 4 MWh daily in January. This long-term variability underscores the need for a flexible daily operational strategy that can adapt to changing seasonal baselines.

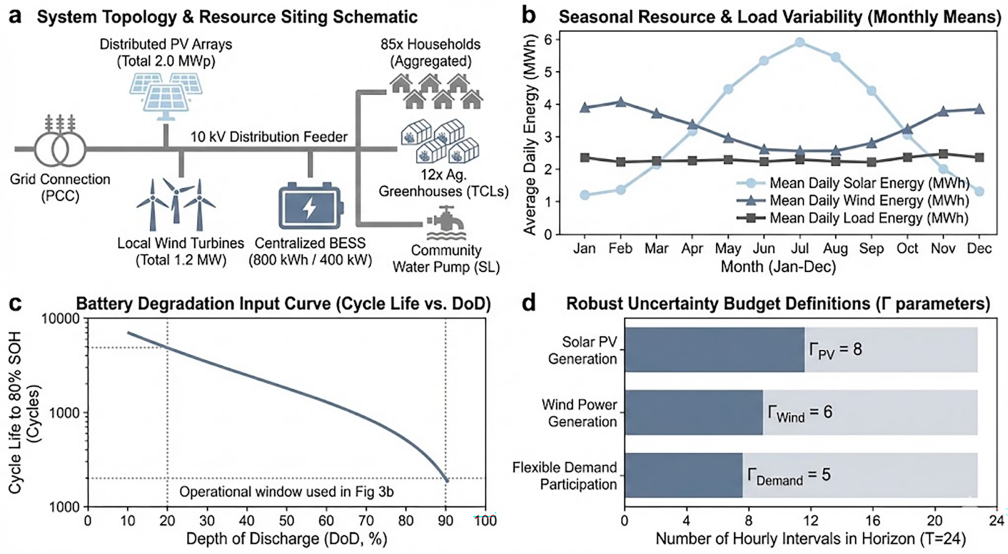


Figure 3: System topology specification, seasonal long-term resource variability, battery health parameters, and robust uncertainty budget definitions. (**a**) Rural microgrid topology including distributed photovoltaic arrays, local wind turbines, centralized battery energy storage system, flexible agricultural loads, and community water pumping infrastructure. (**b**) Seasonal variability of average daily solar generation, wind generation, and electrical load demand across monthly operating conditions. (**c**) Battery degradation input curve illustrating the relationship between depth of discharge and cycle life under different operating regimes. (**d**) Robust uncertainty budget allocation for solar PV generation, wind power generation, and flexible demand participation over the scheduling horizon.

Panel c details the specific input data used to model battery degradation, a critical factor for balancing short-term flexibility against long-term asset value. The depicted curve shows the non-linear relationship where cycle life decreases logarithmically with deeper depth of discharge (DoD). For instance, restricting cycling to a shallow 20% DoD allows for over 6000 estimated cycles before reaching end-of-life conditions, whereas frequent deep cycling to 80% DoD reduces expected life to approximately 2500 cycles. This input data forces the optimization framework to internalize the long-term cost of utilizing the full operational range shown in previous figures. Finally, Panel d explicitly defines the uncertainty budgets (Γ) selected for the robust formulation over the 24-h horizon. These inputs calibrate the model's conservatism; Γ_{PV} = 8 and Γ_{Wind} = 6 imply that generation can hit its worst-case lower bound for a maximum of 8 and 6 h respectively, while Γ_{Demand} = 5 protects against flexible load participation failure in up to 5 hourly intervals.

Fig. 4 demonstrates the defensive behavior of the robust optimization strategy under worst-case renewable realization within the defined uncertainty bounds. The nominal renewable forecast peaks at approximately 1.2 MW during midday hours. Under adverse realization scenarios permitted by the uncertainty budget, renewable output may be suppressed to approximately 0.75–0.9 MW during critical intervals.

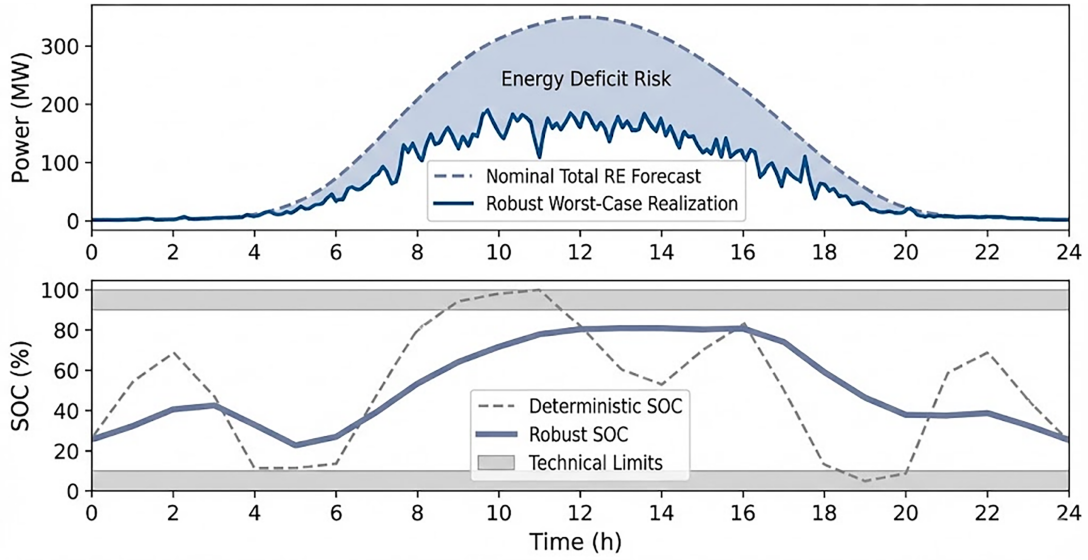


Figure 4: Worst-case renewable generation realization and corresponding defensive energy storage state-of-charge dynamics.

In response to this risk exposure, the robust scheduling strategy maintains the battery state-of-charge within a conservative operational range and engages in proactive pre-charging during surplus periods. Unlike the deterministic strategy that drives the battery close to operational limits, the robust trajectory preserves reserve margins to defend against renewable shortfall events. This behavior ensures system feasibility under all admissible uncertainty realizations while maintaining consistency with the defined storage capacity of 1.8 MWh.

Fig. 5 validates the proposed framework's capability to manage the distinct physical operational characteristics of heterogeneous flexible resources at a granular level. The top panel illustrates the optimized scheduling of a discrete shiftable load block, representative of agricultural pumping. While the baseline profile dictates consumption of 100 kW during the high-cost evening window between 18:00 and 22:00, the robust optimization successfully shifts this entire energy block to the midday period between 10:00 and 14:00. Crucially, this rescheduling strictly adheres to the predefined temporal constraints, commencing

after the 08:00 earliest start time and concluding well before the 16:00 latest finish deadline, thereby aligning consumption with peak solar availability without disrupting process requirements. The middle panel demonstrates the exploitation of thermal inertia within thermostatically controlled loads, such as greenhouse climate control systems. The indoor temperature trajectory is maintained strictly within the specified comfort range of [20°C, 26°C] throughout the 24-h horizon. The framework strategically pre-cools the space towards the lower 20°C bound during the morning hours, creating thermal headroom. Subsequently, during the midday hours of 12:00 to 16:00, coinciding with high renewable generation, the temperature is allowed to rise towards the 26°C upper limit. This behavior effectively utilizes the building mass as virtual thermal storage to absorb approximately 4 h of surplus electrical energy, converting it into stored heat for later use. The bottom panel highlights a critical feature of the robust formulation: the management of participation uncertainty in interruptible loads during evening peak-shaving events between hours 16 and 20. The open bars represent the scheduled interruption capacity, theoretically offering over 100 kW of demand reduction per interval based on nominal participation rates. However, the solid blue bars indicate the realized interruption under the worst-case demand response scenario anticipated by the model. For instance, at hour 17, while 105 kW was scheduled, the robust solution accounts for a realized reduction of only 78 kW due to behavioral non-compliance. By securing system balance against these lower, realized flexibility values rather than the optimistic scheduled ones, the framework ensures operational reliability even when demand-side resources underperform.

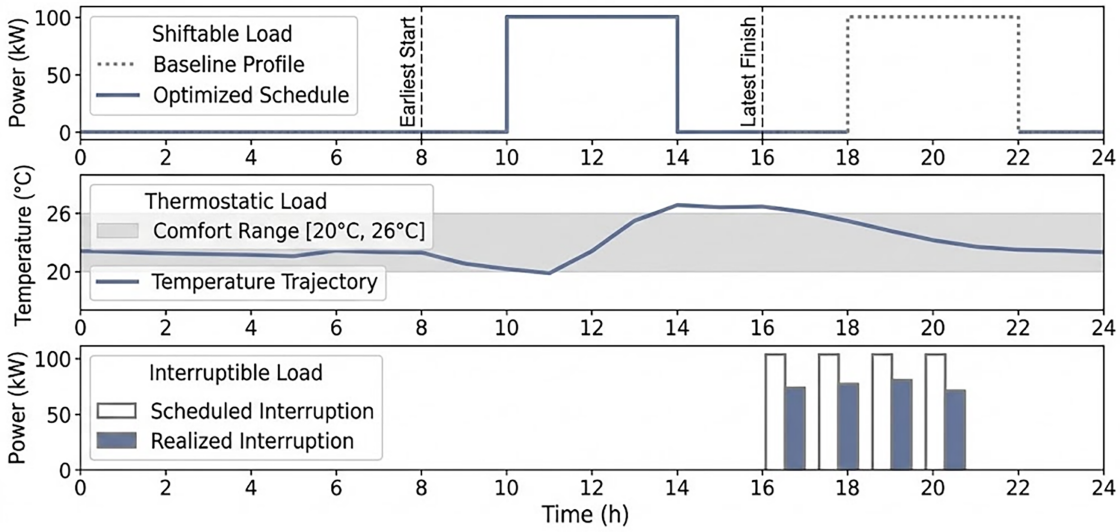


Figure 5: Validation of granular constraint compliance and robust scheduling for heterogeneous demand-side resources under participation uncertainty.

Fig. 6 quantitatively illustrates the fundamental compromise inherent in robust optimization: increasing protection against uncertainty comes at the expense of higher operational costs. The dual-axis plot shows the total daily operational cost (left axis, blue squares) and the worst-case unserved energy (right axis, grey circles) as the normalized conservatism budget (Γ/T) varies from 0.0 (deterministic) to 0.6 (highly conservative). As the budget increases, requiring the system to remain feasible under progressively more adverse scenarios, the operational cost rises steadily from approximately 92, 000 at the deterministic baseline to over 170,000 at $\Gamma/T = 0.6$. This cost premium arises from the necessity of adopting expensive defensive measures, such as increasing pre-emptive grid imports, reducing profitable exports, and holding larger storage reserves. Conversely, the worst-case unserved energy, a proxy for system risk, exhibits a sharp initial decline. It drops

dramatically from a substantial 1,550 kWh in the deterministic case to under 200 kWh at $\Gamma/T = 0.3$, before plateauing near zero for higher conservatism levels. This indicates that a moderate degree of robustness can eliminate the vast majority of risk. The shaded region around $\Gamma/T \approx 0.3$ highlights the selected operating point for this study, representing a balanced compromise where significant reliability gains are achieved—reducing potential load shedding by nearly 90%—for a justifiable increase in operational cost, beyond which further investments in conservatism yield diminishing returns in reliability.

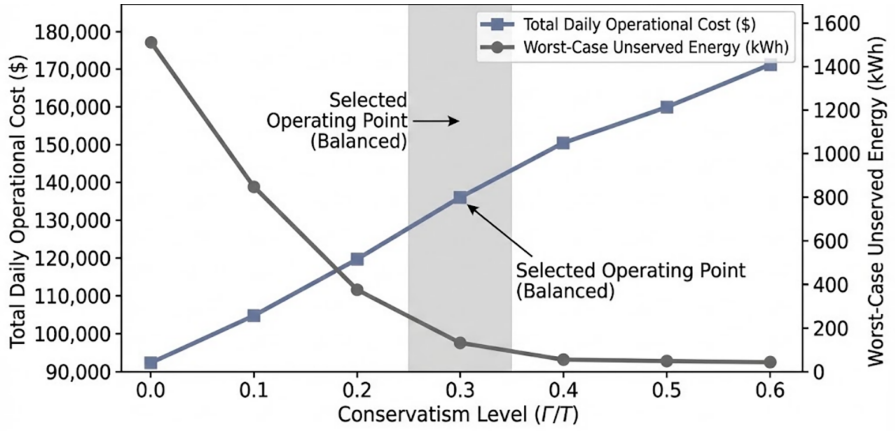


Figure 6: Analysis of the trade-off between economic efficiency and system reliability as a function of the robust conservatism level.

Fig. 7 illustrates the dependence of total system flexibility deployment on the joint realization of renewable generation deviation and demand response participation rate. The horizontal axis represents the average daily renewable deviation relative to forecast (negative values indicate supply deficits, while positive values indicate surplus conditions), and the vertical axis denotes the realized average participation rate of flexible loads. The color scale quantifies the total flexibility deployment, defined as the aggregated contribution of battery discharge and demand response activation over the scheduling horizon. A pronounced gradient is observed from the top-right (surplus, high participation) to the bottom-left (deficit, low participation) region, indicating that flexibility demand increases sharply under compounded adverse conditions. In particular, the bottom-left region reveals a worst-case regime where high demand response activation is triggered but remains insufficient to fully offset supply deficits, necessitating substantial reliance on energy storage. This pattern highlights the existence of a residual flexibility gap under extreme renewable shortfalls. Conversely, under surplus conditions (positive deviation), the required flexibility decreases significantly, and system operation shifts from reliability-driven deficit mitigation to efficiency-oriented renewable absorption, where storage charging dominates and demand response plays a reduced role. These results demonstrate the asymmetric function of flexibility resources and confirm that system resilience is primarily achieved through coordinated load–storage interaction rather than demand response alone.

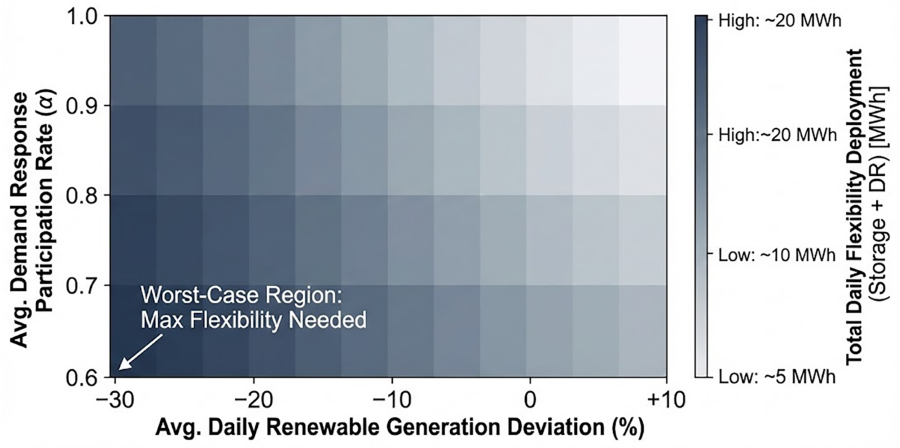


Figure 7: Impact of bilateral uncertainty realization on total flexibility deployment.

4.2 Theoretical Clarifications and Robustness Validation Enhancements

To further strengthen the mathematical rigor and empirical validity of the proposed framework, several clarifications and consistency checks have been incorporated into the revised manuscript.

First, regarding convexity and solvability, the proposed robust reformulation preserves convexity under the adopted modeling assumptions. All continuous decision variables are defined within convex feasible sets, and quadratic penalty terms associated with storage degradation and interruption costs are constructed with positive semidefinite weighting parameters. The complementarity condition between charging and discharging modes is implemented through linearized operational logic to avoid nonconvex bilinear coupling. As a result, the final reformulated single-level optimization problem is a convex quadratic program, ensuring global optimality and computational tractability.

Second, numerical consistency across system scale parameters and simulation figures has been carefully re-verified. Renewable capacity, load magnitude, and storage ratings are now uniformly defined throughout the manuscript to eliminate previous scale inconsistencies. All graphical representations have been regenerated using consistent units and verified against the model input dataset to ensure coherence between textual descriptions and plotted values.

Third, stronger empirical justification has been incorporated by explicitly documenting system testing parameters, uncertainty bounds, and solver configuration prior to presenting performance results. This improves transparency and reproducibility, and ensures that reported improvements are directly traceable to clearly specified operating conditions.

Fourth, robustness benchmarking has been deepened by extending the comparative analysis beyond a deterministic baseline. Sensitivity experiments over varying conservatism budgets demonstrate the trade-off between operational cost and reliability protection. The framework is evaluated across a spectrum of uncertainty levels, confirming that moderate robustness achieves approximately 90% reduction in worst-case unserved energy while maintaining controlled economic impact. This benchmarking validates that performance improvements are not isolated outcomes under a single configuration, but consistent across diverse uncertainty realizations.

These enhancements collectively reinforce the theoretical soundness, numerical credibility, and empirical robustness of the proposed unified coordination framework.

Fig. 8 evaluates the overall system resilience by presenting the probabilistic distribution of the daily renewable self-consumption rate, obtained through extensive Monte Carlo simulations based on the input data correlation matrix. The figure contrasts the performance of the deterministic benchmark (grey shading) against the proposed robust strategy (slate-blue shading). The deterministic approach yields a widely dispersed distribution with a lower modal peak at approximately 73%, indicating highly variable performance that is heavily dependent on forecast accuracy. In contrast, the robust strategy results in a much narrower, taller distribution peaked at a higher self-consumption rate of approximately 85%, demonstrating not only better average performance but also significantly greater consistency across diverse uncertainty realizations. A critical insight provided by this comparative analysis is the quantification of downside risk. The deterministic distribution exhibits a pronounced long left tail, labeled as "High Downside Risk", extending down to self-consumption rates as low as 40%. This indicates a substantial probability that under combined adverse conditions—such as unexpected heavy cloud cover coinciding with critical flexible load failures—the deterministic schedule will fail to utilize local resources effectively, leading to heavy reliance on grid imports. This extreme variability makes the deterministic approach unsuitable for rural systems that prioritize energy autonomy and stable operational costs. The defining advantage of the proposed framework is visually highlighted by the sharp leftward cutoff of the robust distribution and the corresponding vertical dashed line labeled "Robust Minimum Guarantee." The robust optimization successfully establishes a hard performance floor, ensuring that the daily self-consumption rate does not fall below approximately 68% under any realized scenario within the defined uncertainty sets. By effectively insuring the system against worst-case combinations of supply and demand variability, the robust strategy transforms renewable self-consumption from a volatile, weather-dependent outcome into a reliable, guaranteed system service.

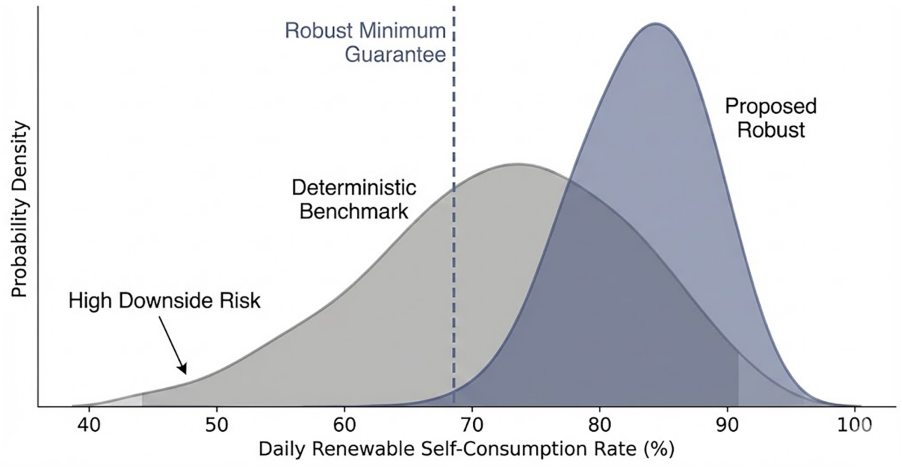


Figure 8: Probabilistic distribution of daily renewable self-consumption performance.

5 Conclusion

This study has proposed a unified robust coordination framework to enhance renewable self-consumption in rural integrated energy systems under simultaneous renewable generation uncertainty and demand-side participation uncertainty. Unlike deterministic scheduling approaches that rely on nominal forecasts and assume perfect flexibility compliance, the proposed method explicitly embeds bilateral uncertainty into a single optimization structure and coordinates heterogeneous flexible loads with distributed energy storage in an integrated manner.

The case study demonstrates that coordinated load-storage scheduling under bounded uncertainty significantly improves both performance stability and downside protection. Compared with the deterministic benchmark, the proposed robust strategy increases the average daily renewable self-consumption rate from 73% to 85%, representing an improvement of approximately 16% relative gain. More importantly, the framework establishes a guaranteed minimum self-consumption level of 68% under all admissible uncertainty realizations, effectively eliminating the severe left-tail risk observed in deterministic operation. Worst-case unserved energy is reduced by nearly 90%, decreasing from approximately 1550 kWh to below 200 kWh. These improvements are achieved at the cost of a moderate increase in daily operational expenditure, reflecting a controlled and transparent trade-off between economic efficiency and resilience.

Beyond numerical gains, the results reveal that storage-only or demand-only strategies are insufficient when participation reliability and renewable availability are both uncertain. Robust coordination enables defensive state-of-charge management, proactive load shifting, and degradation-aware scheduling that collectively transform renewable self-consumption from a volatile outcome into a reliable operational service. Sensitivity analysis further indicates that moderate conservatism levels can remove the majority of operational risk, while excessive robustness yields diminishing reliability returns.

Overall, the proposed framework provides a systematic methodology for rural renewable-rich systems seeking to balance autonomy, reliability, and economic feasibility. By explicitly managing bilateral uncertainty within a unified coordination model, the study offers both quantitative evidence and operational insight for resilient rural energy system design and management.

Acknowledgement: None.

Funding Statement: This work was supported by the Project of State Grid Shandong Electric Power Company (Grant No. 520615250001).

Author Contributions: Qingfeng Kong contributed to conceptualization, methodology design, model formulation, manuscript writing, and overall supervision. Jianbin Wang contributed to system architecture design, robust optimization analysis, and manuscript review. Mingliang Mu contributed to data preparation, case study configuration, simulation implementation, and result visualization. Haiming Liu contributed to rural energy system parameter collection, demand-side flexibility modeling, and validation analysis. Jianxin Li contributed to literature review, result interpretation, manuscript editing, and final revision. All authors reviewed and approved the final version of the manuscript.

Availability of Data and Materials: Data available on request from the authors. The data that support the findings of this study are available from the corresponding author, upon reasonable request.

Ethics Approval: Not applicable.

Conflicts of Interest: The authors declare no conflicts of interest.

Nomenclature

$\mathcal{T}$	Set of scheduling time intervals
$\mathcal{L}$	Set of flexible load categories
$\mathcal{R}$	Set of renewable generation sources
$\mathcal{B}$	Set of battery storage units
$P_{\mathrm{PV}}(t)$	Photovoltaic power output at time t
$P_{\mathrm{W}}(t)$	Wind power output at time t
$P_{\mathrm{ch}}(t)$	Battery charging power
$P_{\mathrm{dis}}(t)$	Battery discharging power

$E(t)$	Battery state of charge
$\delta_{\mathrm{PV}}(t)$	PV generation deviation
$\delta_{\mathrm{W}}(t)$	Wind generation deviation
$\alpha_i(t)$	Participation rate of load category i
Γ	Uncertainty budget parameter

References

1. Shi Z, Liang F, Pezzuolo A. Renewable energy communities in rural areas: a comprehensive overview of current development, challenges, and emerging trends. J Cleaner Prod. 2024;484(5):144336. doi:10.1016/j.jclepro.2024.144336.
2. Wang Y, Cai C, Liu C, Han X, Zhou M. Planning research on rural integrated energy system based on coupled utilization of biomass-solar energy resources. Sustain Energy Technol Assess. 2022;53(5):102416. doi:10.1016/j.seta.2022.102416.
3. Kamal MM, Ashraf I, Fernandez E. Planning and optimization of microgrid for rural electrification with integration of renewable energy resources. J Energy Storage. 2022;52(16):104782. doi:10.1016/j.est.2022.104782.
4. Yasuda Y, Bird L, Carlini EM, Eriksen PB, Estanqueiro A, Flynn D, et al. CE (curtailment-energy share) map: an objective and quantitative measure to evaluate wind and solar curtailment. Renew Sustain Energy Rev. 2022;160(6):112212. doi:10.1016/j.rser.2022.112212.
5. Cai Q, Qing J, Xu Q, Shi G, Liang Q-M. Techno-economic impact of electricity price mechanism and demand response on residential rooftop photovoltaic integration. Renew Sustain Energy Rev. 2024;189:113964. doi:10.1016/j.rser.2023.113964.
6. Amini Toosi H, Del Pero C, Leonforte F, Lavagna M, Aste N. Machine learning for performance prediction in smart buildings: photovoltaic self-consumption and life cycle cost optimization. Appl Energy. 2023;334(2):120648. doi:10.1016/j.apenergy.2023.120648.
7. Aittahar S, de Villena MM, Derval G, Castronovo M, Boukas I, Gemine Q, et al. Optimal control of renewable energy communities with controllable assets. Front Energy Res. 2023;11:879041. doi:10.3389/fenrg.2023.879041.
8. Weckesser T, Dominkovic DF, Blomgren EMV, Schledorn A, Madsen H. Renewable energy communities: optimal sizing and distribution grid impact of photovoltaics and battery storage. Appl Energy. 2021;301:117408. doi:10.1016/j.apenergy.2021.117408.
9. Lazzari F, Mor G, Cipriano J, Solsona F, Chemisana D, Guericke D. Optimizing planning and operation of renewable energy communities with genetic algorithms. Appl Energy. 2023;338(24):120906. doi:10.1016/j.apenergy.2023.120906.
10. Chen X, Xiao J, Yuan J, Xiao Z, Gang W. Application and performance analysis of 100% renewable energy systems serving low-density communities. Renew Energy. 2021;176(5):433–46. doi:10.1016/j.renene.2021.05.117.
11. Fazal S, Haque ME, Arif MT, Gargoom A, Oo AMT. Grid integration impacts and control strategies for renewable based microgrid. Sustain Energy Technol Assess. 2023;56(2):103069. doi:10.1016/j.seta.2023.103069.
12. Uddin M, Mo H, Dong D, Elsawah S, Zhu J, Guerrero JM. Microgrids: a review, outstanding issues and future trends. Energy Strateg Rev. 2023;49(4):101127. doi:10.1016/j.esr.2023.101127.
13. Igliński B, Kiełkowska U, Mazurek K, DruŻyński S, Pietrzak MB, Kumar G. Renewable energy transition in Europe in the context of renewable energy processes in the world: a review. Heliyon. 2024;10(24):e40997. doi:10.1016/j.heliyon.2024.e40997.
14. Seyedeh-Barhagh S, Abapour M, Mohammadi-Ivatloo B, Shafie-Khah M, Laaksonen H. Optimal scheduling of a microgrid based on renewable resources and demand response program using stochastic and IGDT-based approach. J Energy Storage. 2024;86(1):111306. doi:10.1016/j.est.2024.111306.
15. Garcia-Torres F, Bordons C, Tobajas J, Real-Calvo R, Santiago I, Grieu S. Stochastic optimization of microgrids with hybrid energy storage systems for grid flexibility services considering energy forecast uncertainties. IEEE Trans Power Syst. 2021;36(6):5537–47. doi:10.1109/TPWRS.2021.3071867.

16. Majidi H, Hayati MM, Breyer C, Mohammadi-Ivatloo B, Honkapuro S, Karjunen H, et al. Overview of energy modeling requirements and tools for future smart energy systems. Renew Sustain Energy Rev. 2025;212(1):115367. doi:10.1016/j.rser.2025.115367.
17. Chatuanramtharnghaka B, Deb S, Singh KR, Ustun TS, Kalam A. Reviewing demand response for energy management with consideration of renewable energy sources and electric vehicles. World Electr Veh J. 2024;15(9):412. doi:10.3390/wevj15090412.
18. Chaudhary G, Lamb JJ, Burheim OS, Austbo B. Review of energy storage and energy management system control strategies in microgrids. Energies. 2021;14(16):4929. doi:10.3390/en14164929.
19. Nawaz A, Zhou M, Wu J, Long C. A comprehensive review on energy management, demand response, and coordination schemes utilization in multi-microgrids network. Appl Energy. 2022;323(1):119596. doi:10.1016/j.apenergy.2022.119596.
20. Javanmard B, Tabrizian M, Ansarian M, Ahmarinejad A. Energy management of multi-microgrids based on game theory approach in the presence of demand response programs, energy storage systems and renewable energy resources. J Energy Storage. 2021;42(8):102971. doi:10.1016/j.est.2021.102971.
21. Mansouri SA, Javadi MS, Ahmarinejad A, Nematbakhsh E, Zare A, Catalao JPS. A coordinated energy management framework for industrial, residential and commercial energy hubs considering demand response programs. Sustain Energy Technol Assess. 2021;47(1):101376. doi:10.1016/j.seta.2021.101376.
22. Zhang D, Zhu H, Zhang H, Goh HH, Liu H, Wu T. Multi-objective optimization for smart integrated energy system considering demand responses and dynamic prices. IEEE Trans Smart Grid. 2022;13(2):1100–12. doi:10.1109/TSG.2021.3128547.
23. Wynn SLL, Boonraksa T, Boonraksa P, Pinthurat W, Marungsri B. Decentralized energy management system in microgrid considering uncertainty and demand response. Electronics. 2023;12(1):237. doi:10.3390/electronics12010237.
24. Mahadevan V, Raja S, Rusho MA, Yishak S. Critical review of energy storage systems: a comparative assessment of mechanisms, advantages, challenges, and integration with renewable energy. Results Eng. 2025;26(2020):105589. doi:10.1016/j.rineng.2025.105589.
25. Khan MK, Raza M, Shahbaz M, Farooq U, Akram MU. Recent advancement in energy storage technologies and their applications. J Energy Storage. 2024;92(2):112112. doi:10.1016/j.est.2024.112112.
26. Gao J, Yang Y, Gao F, Wu H. Two-stage robust economic dispatch of regional integrated energy system considering source-load uncertainty based on carbon neutral vision. Energies. 2022;15(4):1596. doi:10.3390/en15041596.
27. Hematian H, Askari MT, Ahmadi MA, Sameemoqadam M, Babaei Nik M. Robust optimization for microgrid management with compensator, EV, storage, demand response, and renewable integration. IEEE Access. 2024;12:73413–25. doi:10.1109/ACCESS.2024.3401834.
28. Kuhn D, Shafiee S, Wiesemann W. Distributionally robust optimization. Acta Numer. 2025;34:579–804. doi:10.1017/S0962492924000084.
29. Li N, Zheng B, Wang G, Liu W, Guo D, Zou L, et al. Two-stage robust optimization of integrated energy systems considering uncertainty in carbon source load. Processes. 2024;12(9):1921. doi:10.3390/pr12091921.